

Grain Boundary Motion on Curved Substrate

Kongtao Chen

Department of Materials Science and NanoEngineering, Rice University, Houston, TX 77005 USA

Abstract

Grain boundary (GB) kinetics is important for many applications in 2d materials and metal thin films. To study how the substrate shape affects GB mobility and kinetics, we develop a kinetic Monte-Carlo (kMC) simulation method and an analytical model for GBs on the curved substrate by combining disconnection theory and by Föppl–von Kármán equations. Using sinusoidal MoS₂ as an example, we can increase its GB mobility more than 50 times by changing substrate shape amplitudes and periods. We find that amplitude change GB mobility exponentially while wave vector change GB mobility linearly. The sinusoidal GB kinetic shape has wave vector twice as substrate and amplitude proportional to substrate squared amplitude.

Introduction

Grain boundary (GB) kinetics is important for many applications in 2d materials¹ and metal thin films². GB motions are used to absorb stacking faults and rotational disorders in 2d transition metal dichalcogenides (TMDs)³. Polycrystalline molybdenum disulfide (MoS₂) cracks along GB⁴ if GBs don't move and stress accumulates. GB orientations, which affect mechanical properties⁵, failure modes¹, electric transport⁶ of 2d TMDs, may change when GB migrates. GB motions are also observed in polycrystalline MoS₂ memtransistors⁷. The single-crystal metal substrate useful for the growth of single-crystal TMDs is often processed by grain growth². The dynamics of flat GBs in 2d materials have been studied by dislocation dynamics^{8–15} and molecular dynamics simulations¹⁶. How substrate shape affects GB dynamics, however, hasn't been studied yet.

A disconnection-based model^{17–24} for GB motion in bulk materials was recently developed to systematically and quantitatively explain many GB properties, e.g., shear coupling^{18–20}, mobility^{20,21}, sliding²⁰, roughening²² and phase transitions²². This disconnection-based model was recently applied on GBs in 2d materials^{25,26}, which was traditionally regarded as arrays of dislocations¹.

We develop a disconnection-based kinetic Monte-Carlo (kMC) simulation method for GBs on curved substrate to study how the substrate shape affects GB mobility and kinetic shapes. The stress and strain fields are calculated by Föppl–von Kármán equations^{27–29}.

Methods

We first determine the stress and strain fields from Föppl–von Kármán equations^{27–29}, and then perform the kMC simulations proposed by Chen et al.²¹ Assume the 2d material (and substrate) has a periodic shape

$$z = \frac{c}{\alpha} \sin \alpha x \sin \alpha y \quad (1)$$

Where x , y , and z are defined in Figure 1. When strain is small ($c \ll 1$), Föppl–von Kármán equations^{27–29} leads to strain field

$$\epsilon_{xx} = \frac{c^2}{8} (\nu \cos 2\alpha x - \cos 2\alpha y) \quad (2)$$

$$\epsilon_{yy} = \frac{c^2}{8} (\nu \cos 2\alpha y - \cos 2\alpha x) \quad (3)$$

Where ν is Poisson's ratio. The shear stress $\sigma_{xy} = 0$. The disconnection Burgers vector b and step height h at different locations will rescale with ϵ_{xx} and ϵ_{yy} , respectively.

In the kMC simulation (See Figure 1), each event corresponds to changes in the disconnections of mode m at site i ; the associated barrier ΔE_{im} is determined by the constant glide barrier and the change in energy of the state after the occurrence of the event. The rate of such an event is proportional to $\exp(-\Delta E_{im}/k_B T)$. At each kMC step, we randomly choose one event from a list of all possible events (weighted by their rates), execute that event, and advance the clock in accordance with the sum of the rate of all possible events. GB motion is driven by a chemical potential jump ψ across GB. A more detailed description of the kinetic Monte Carlo method is in Chen et al.²¹ We set GB energy $\gamma = 1 \text{ J/m}^2$, temperature $T = 1500 \text{ K}$, and use the material parameters of MoS_2 (lattice constant $a = 0.32 \text{ nm}$, thickness $w = 1.23 \text{ nm}$, shear modulus $G = 50 \text{ GPa}$, Poisson's ratio $\nu = 0.25$)^{30–32}.

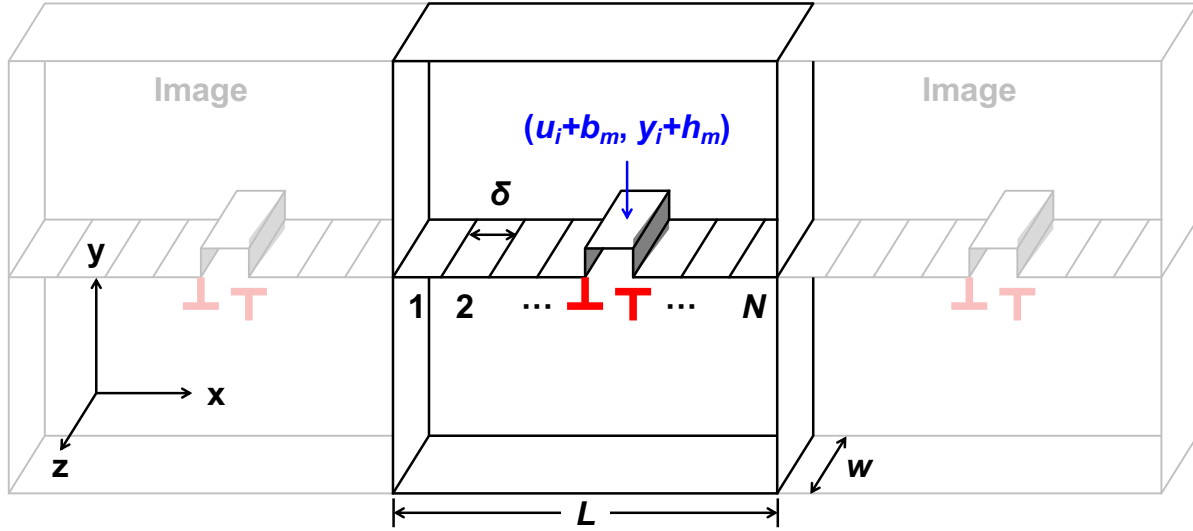


Figure 1 Disconnection dipoles on a 1d GB in 2d materials. δ , w , and L denote the disconnection core size, thickness of the material, and the system size in the y -direction, respectively. The states of the system at i before and after disconnection dipole nucleation are (u_i, z_i) and $(u_i + b_m, z_i + h_m)$, respectively, for a pair of disconnections of mode m at location i .

Results

Figure 2 shows that the time-averaged kinetic GB shape when migration is a sinusoidal function

$$y \propto c^2 h \sin 2\alpha x \quad (4)$$

The wave vector is the same as ϵ_{xx} and ϵ_{yy} (or twice as substrate). This is because 2α is the wave vector of the whole periodic simulation system. The amplitude $D \propto c^2 h$, also proportional to ϵ_{xx} and ϵ_{yy} .

Figure 3 shows that reduced mobility \tilde{M} (the GB mobility on a substrate described by Equation (1) over the mobility of a flat GB) is proportional to substrate wave vector α , and $\ln \tilde{M}$ is proportional to c . This is because the disconnection nucleation barrier per thickness at any site

$$\frac{Q}{w} = Ab^2(1 + \epsilon_{xx})^2 + 2\gamma|h(1 + \epsilon_{yy})| + C \quad (5)$$

has $N\alpha/\pi$ minima, $Q_{\min}/w = Ab^2[1 - c^2(1 + \nu)/8]^2 + 2\gamma|h(1 - c^2(1 + \nu)/8)|$, where $A = -2G[(1 - \nu \cos^2 \beta)/4\pi(1 - \nu)] \ln \sin(\pi r_0/L)$, G is the shear modulus, ν is the Poisson's ratio, β is the angle between the Burgers vector and the disconnection line direction, and r_0 is the disconnection core size. A describes the energy required to form a dislocation pair and separate it to a distance of half the periodic unit cell $L/2$ and GB energy γ describes the energy required to form a pair of steps¹⁷⁻²³. C represents the disconnection migration barrier which depends on the GB structure and bonding character; this is dominated by core-level phenomena and may be determined via calculations on the atomic scale^{20,33}. Assume disconnections only nucleate at these minimum sites and bulk material parameters (A , γ , C) don't change under small strain, the reduced mobility

$$\tilde{M} = \frac{M(\alpha, c)}{M(\alpha = 0, c = 0)} = \frac{N\alpha}{\pi} \exp \left[\frac{(Ab^2 + 2\gamma h)c^2(1 + \nu)w}{4k_B T} + O(c^4) \right] \quad (6)$$

This result is consistent with simulation results in Figure 3.

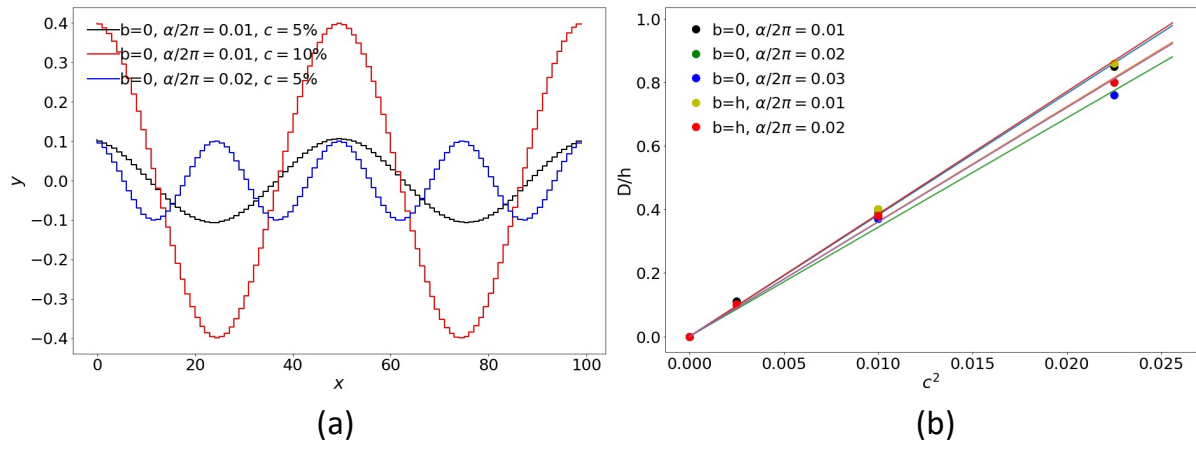


Figure 2 Kinetic GB shapes on curved 2d materials. The time-averaged kinetic GB shape when migration is a sinusoidal function with twice the same wave vector as substrate and amplitude $D \propto c^2$.

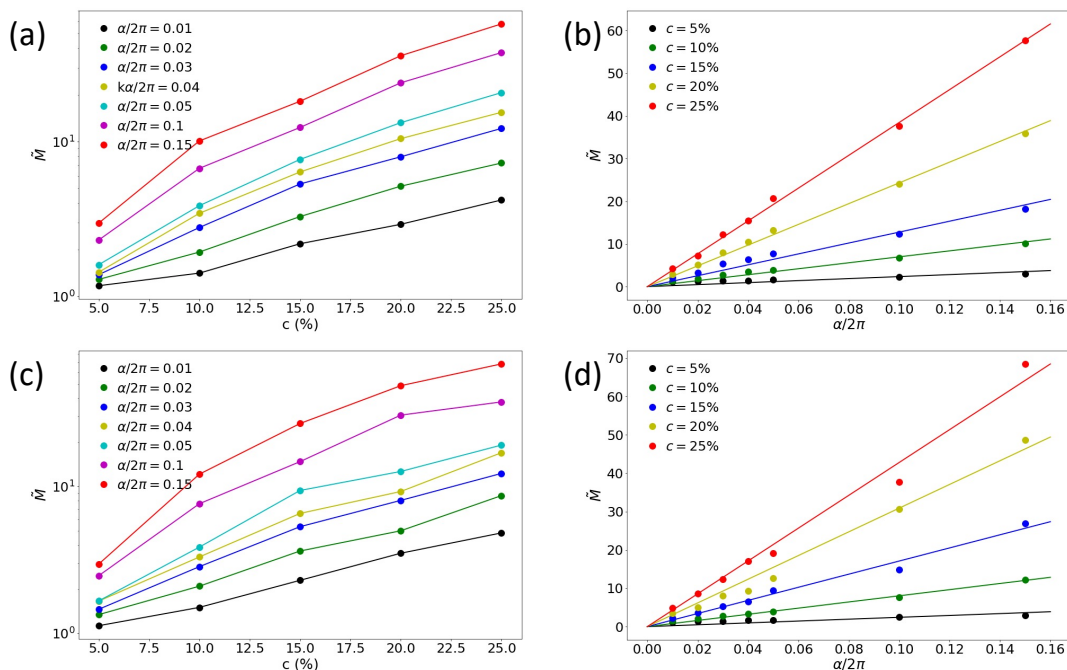


Figure 3 GB mobility as a function of substrate shape. Reduced mobility \tilde{M} is the GB mobility on a substrate described by Equation (1) over the mobility of a flat GB. The disconnection mode in (a) and (b) is $b = 0$, $h = a$; the mode in (c) and (d) is $b = h = a$.

Conclusion

We develop a kMC simulation method and analytical model for GB kinetics of 2d materials on non-uniform substrates, by combining disconnection theory and by Föppl–von Kármán equations. Using MoS₂ as an example, we can increase its GB mobility for > 50 times by changing substrate shape amplitudes and periods. We find that amplitude change GB mobility exponentially while wave vector change GB mobility linearly. The sinusoidal GB kinetic shape has wave vector twice as substrate and amplitude proportional to substrate squared amplitude.

Reference

1. Man, P., Srolovitz, D., Zhao, J. & Ly, T. H. Functional Grain Boundaries in Two-Dimensional Transition-Metal Dichalcogenides. *Acc. Chem. Res.* acs.accounts.1c00519 (2021). doi:10.1021/acs.accounts.1c00519

2. Thompson, C. V. Grain growth in thin films. *Annu. Rev. Mater. Sci.* **20**, 245–268 (1990).
3. Zhao, X. *et al.* Healing of Planar Defects in 2D Materials via Grain Boundary Sliding. *Adv. Mater.* **31**, 1900237 (2019).
4. Wu, J. *et al.* Grain-Size-Controlled Mechanical Properties of Polycrystalline Monolayer MoS₂. *Nano Lett.* **18**, 1543–1552 (2018).
5. Wu, J. *et al.* Topology and polarity of dislocation cores dictate the mechanical strength of monolayer MoS₂. *Appl. Mater. Today* **15**, 34–42 (2019).
6. Ly, T. H. *et al.* Misorientation-angle-dependent electrical transport across molybdenum disulfide grain boundaries. *Nat. Commun.* **7**, 1–7 (2016).
7. Sangwan, V. K. *et al.* Multi-terminal memtransistors from polycrystalline monolayer molybdenum disulfide. *Nature* **554**, 500–504 (2018).
8. Kurasch, S. *et al.* Atom-by-atom observation of grain boundary migration in graphene. *Nano Lett.* **12**, 3168–3173 (2012).
9. Gong, C., He, K., Chen, Q., Robertson, A. W. & Warner, J. H. In Situ High Temperature Atomic Level Studies of Large Closed Grain Boundary Loops in Graphene. *ACS Nano* **10**, 9165–9173 (2016).
10. Azizi, A. *et al.* Dislocation motion and grain boundary migration in two-dimensional tungsten disulphide. *Nat. Commun.* **5**, 1–7 (2014).
11. Kim, D., Kim, Y., Ihm, J., Yoon, E. & Lee, G. Do. Atomic-scale mechanism of grain boundary motion in graphene. *Carbon N. Y.* **84**, 146–150 (2015).
12. Lee, G. Do, Yoon, E., Wang, C. Z. & Ho, K. M. Atomistic processes of grain boundary motion and annihilation in graphene. *J. Phys. Condens. Matter* **25**, 155301 (2013).
13. Wang, J., Li, S. N. & Liu, J. B. Migrations of pentagon-heptagon defects in hexagonal boron nitride monolayer: The first-principles study. *J. Phys. Chem. A* **119**, 3621–3627 (2015).
14. Taha, D., Mkhonta, S. K., Elder, K. R. & Huang, Z. F. Grain Boundary Structures and Collective Dynamics of Inversion Domains in Binary Two-Dimensional Materials. *Phys. Rev. Lett.* **118**, 255501 (2017).
15. Gibb, A. L. *et al.* Atomic resolution imaging of grain boundary defects in monolayer chemical vapor deposition-grown hexagonal boron nitride. *J. Am. Chem. Soc.* **135**, 6758–6761 (2013).
16. Liu, X., Yu, Z. G., Zhang, G. & Zhang, Y. W. Remarkably high thermal-driven MoS₂ grain boundary migration mobility and its implications on defect healing. *Nanoscale* **12**, 17746–17753 (2020).
17. Han, J., Thomas, S. L. & Srolovitz, D. J. Grain-boundary kinetics: A unified approach. *Prog. Mater. Sci.* **98**, 386–476 (2018).
18. Thomas, S. L., Chen, K., Han, J., Purohit, P. K. & Srolovitz, D. J. Reconciling grain growth and shear-coupled grain boundary migration. *Nat. Commun.* **8**, 1–12 (2017).
19. Chen, K., Han, J., Thomas, S. L. & Srolovitz, D. J. Grain Boundary Shear Coupling is Not a Grain Boundary Property. *Acta Mater.* (2019). doi:10.1016/j.ACTAMAT.2019.01.040
20. Chen, K., Han, J., Pan, X. & Srolovitz, D. J. The grain boundary mobility tensor. *Proc. Natl. Acad. Sci. U. S. A.* **117**, 4533–4538 (2020).
21. Chen, K., Han, J. & Srolovitz, D. J. On the Temperature Dependence of Grain Boundary Mobility. *Acta Mater.* **194**, 412–421 (2020).

22. Chen, K., Srolovitz, D. J. & Han, J. Grain-Boundary Topological Phase Transitions. *Proc. Natl. Acad. Sci.* **117**, 33077–33083 (2020).
23. Kaufman, T. *et al.* Disconnection-mediated twin junction migration mechanism in FCC metals. *Microsc. Microanal.* **27**, 3100–3102 (2021).
24. Xu, M. *et al.* Disconnection-Mediated Twin/Twin-Junction Migration in FCC metals. *arXiv*. 2201.04190 (2022).
25. Annevelink, E., Ertekin, E. & Johnson, H. T. Grain boundary structure and migration in graphene via the displacement shift complete lattice. *Acta Mater.* **166**, 67–74 (2019).
26. Ren, X. & Jin, C. Grain boundary motion in two-dimensional hexagonal boron nitride. *ACS Nano* **14**, 13512–13523 (2020).
27. Föppl, A. Vorlesungen über technische Mechanik. in *B.G. Teubner, Bd. 5*. 132 (1907).
28. Kármán, T. V. Festigkeitsprobleme im Maschinenbau. in *Encyk. D. Math. Wiss. IV* 311–385 (1910). doi:10.1007/978-3-663-16028-1_5
29. Landau, L. D. & Lifshitz, E. M. *Course of Theoretical Physics. Course of Theoretical Physics* (Elsevier, 2013). doi:10.1016/c2013-0-00704-9
30. Li, J., Medhekar, N. V. & Shenoy, V. B. Bonding charge density and ultimate strength of monolayer transition metal dichalcogenides. *J. Phys. Chem. C* **117**, 15842–15848 (2013).
31. Hess, P. Prediction of mechanical properties of 2D solids with related bonding configuration. *RSC Adv.* **7**, 29786–29793 (2017).
32. Li, Y. *et al.* Mapping the elastic properties of two-dimensional MoS₂ via bimodal atomic force microscopy and finite element simulation. *npj Comput. Mater.* **4**, 1–8 (2018).
33. Combe, N., Momprou, F. & Legros, M. Disconnections kinks and competing modes in shear-coupled grain boundary migration. *Phys. Rev. B* **93**, 24109 (2016).